

Design of the PROTO-SPHERA experiment and of its first step (MULTI-PINCH)

F. Alladio¹, P. Costa¹, A. Mancuso¹, P. Micozzi¹, S. Papastergiou¹
and F. Rogier²

¹ Associazione EURATOM-ENEA sulla Fusione, CR Frascati, C.P. 65-00044, Frascati, Rome, Italy

² ONERA-CERT/DTIM/M2SN 2, avenue Edouard Belin-BP 4025–31055, Toulouse Cedex 4, France

E-mail: alladio@frascati.enea.it

Received 16 December 2005, accepted for publication 7 April 2006

Published 19 July 2006

Online at stacks.iop.org/NF/46/S613

Abstract

The design study of PROTO-SPHERA, a novel compact torus configuration, has been completed. It is composed of a spherical torus (ST) (with closed flux surfaces) and a force-free screw pinch (SP) (with open flux surfaces and fed by electrodes). PROTO-SPHERA is formed at spherical-tokamak-like densities ($\sim 10^{19} \text{ m}^{-3}$) with low voltage ($\sim 200 \text{ V}$) between the electrodes. The idea of replacing the metal centrepost current (I_{tr}) of the spherical tokamaks with the SP plasma electrode current (I_e) is aimed mainly at getting rid of the rod at the centre of the plasma configuration, which is the most critical component of spherical tokamak design. As a consequence it should be possible to decrease the aspect ratio $A = R/a$ ($R = \text{ST major radius}$, $a = \text{ST minor radius}$) in the course of experiment and to increase the ratio between the toroidal plasma current (I_{ST}) and the plasma electrode current, $I_{\text{ST}}/I_e \gg 1$. Matching two plasma configurations, i.e. an open flux-surface SP and a closed flux-surface ST, brings to life several radically new issues. The purpose of this paper is to analyse the equilibrium, the ideal MHD stability and the formations and modelling issues of such a combined magnetic confinement system. The MULTI-PINCH experimental setup, which is being assembled inside the START vacuum vessel (now in Frascati), will represent the first phase of PROTO-SPHERA: its goal is to prove the feasibility of a stable disc-shaped SP around the electrodes.

PACS numbers: 52.55.Fa, 52.55.Ip, 52.55.–s, 52.55.Tn, 52.35.Vd

(Some figures in this article are in colour only in the electronic version)

1. Introduction

The most investigated and successful magnetic fusion configurations (tokamaks) are doubly connected: a central post, containing the inner part of the toroidal magnet and the ohmic transformer, links the plasma torus. A simply connected magnetic configuration would strongly simplify the design of a fusion reactor, if its confinement properties become as good as those of the doubly connected configurations. The engineering advantages include the simplification of the confining magnetic field (solenoid), the absence of damage and maintenance of the critical central post and the ease of access to a cylindrical reactor chamber. The physics advantages would be even greater if an edge magnetic separatrix with singular magnetic X-points ($\vec{B} = 0$) were present on the symmetry axis at the two ends of the simply connected configuration: a confinement

system with two ‘ends’ could ease the refuelling/exhausting of the plasma and the emerging field lines could help in controlling the electric potential within the plasma [1].

The MHD properties of one such magnetic configuration are considered here. The PROTO-SPHERA system [2], proposed at CR-ENEA Frascati, is a simply connected magnetic configuration, composed of a spherical torus (ST) (with closed flux surfaces and toroidal plasma current I_{ST}) and of a hydrogen plasma arc, in the form of a screw pinch fed by electrodes (SP) (with open flux surfaces and plasma electrode current I_e), (see figure 1). In PROTO-SPHERA the screw pinch replaces the central conductor of a spherical tokamak. Such a combined plasma configuration has been devised theoretically under the name ‘bumpy Z-pinch’ [3] or ‘flux-core-spheromak’ (FCS) [4]. The SP and ST have a common embedded magnetic separatrix (figure 1) with

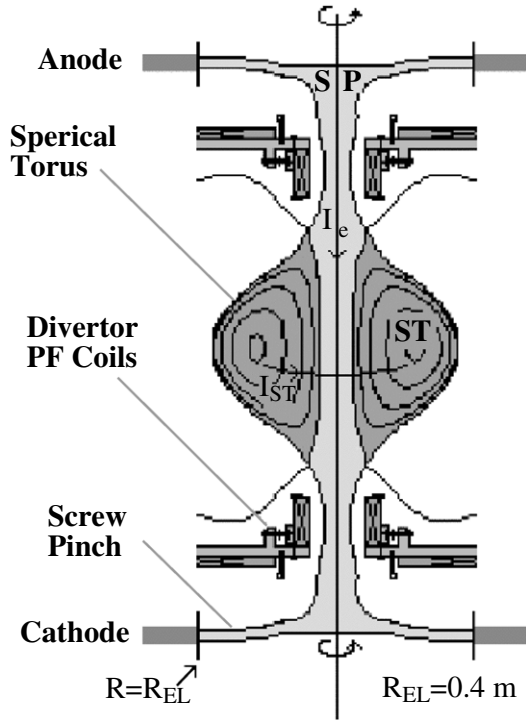


Figure 1. Sketch of the PROTO-SPHERA system.

regular X-points ($\vec{B} \neq 0$): resistive instabilities drive magnetic reconnections, injecting magnetic helicity, poloidal flux and plasma current from the electrode-driven SP into the ST and converting into plasma kinetic energy a fraction of the injected magnetic energy. The SP is magnetically given a disc-shape near each electrode, with a singular magnetic X-point ($\vec{B} = 0$) on the symmetry axis.

The physical bases used in the design of PROTO-SPHERA and of its first step MULTI-PINCH are illustrated, respectively, in sections 2 and 3. The constraints and the assumptions upon the internal plasma profiles, derived from theory and experiments of direct-current helicity injection, are given in detail in section 4. Section 5 introduces the equilibrium calculations, while section 6 works out the equilibria of the formation and compression sequence. Section 7 deals with the ideal MHD stability of PROTO-SPHERA, and finally section 8 concludes with a summary of the paper.

2. The PROTO-SPHERA configuration

2.1. The electrodes

In order to compare the plasma performances of PROTO-SPHERA with those of a spherical tokamak, the geometrical size and the plasma currents of PROTO-SPHERA have been chosen so that they are very similar to the ones that characterized the pioneering spherical tokamak experiment START [5], which was built and operated in Culham from 1991 to 1998. PROTO-SPHERA with an electrode plasma current, $I_e = 60$ kA, produces an elongated ($\kappa = b/a \approx 2.2$ – 2.3) ST of midplane diameter $2R_{sph} \approx 70$ cm, aspect ratio $A \approx 1.2$ – 1.3 , carrying a toroidal current $I_{ST} = 120$ – 240 kA. The screw pinch plasma, of midplane diameter $2\rho_{pinch}(0) \approx 7$ cm, is

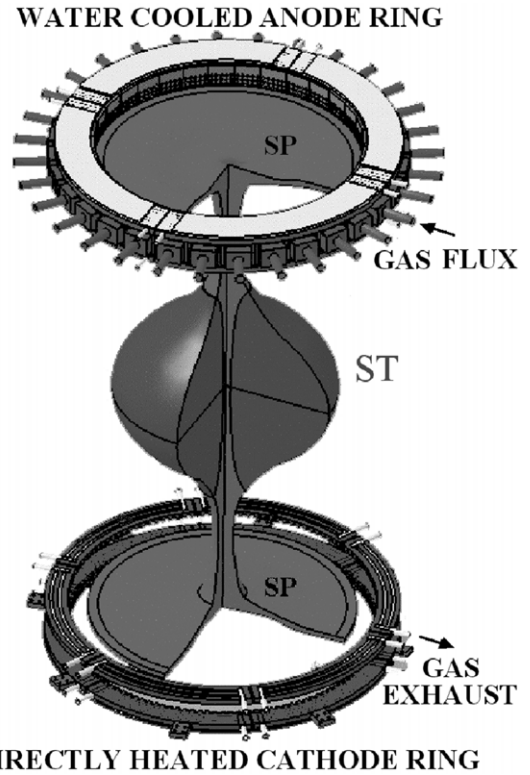


Figure 2. View of the PROTO-SPHERA plasma and electrodes.

magnetically shaped as a disc near each modular ring electrode (see figure 2).

The low voltage (≈ 200 V) electrodes are the most unconventional items of PROTO-SPHERA. They were designed as modular and are composed of a large number of elementary tubes (≈ 600) and wound filaments (≈ 400). The electrodes are made out of refractory metals (hollow gas puffed anodes and directly heated cathodes) and pressed radially into rings: the preliminary PROTO-PINCH electrodes testbench [6] has demonstrated their feasibility.

The main constraint in the physical design of PROTO-SPHERA was the current density at the interface between the SP plasma and the electrodes. In this critical region the maximum electrode plasma current density experimentally demonstrated on PROTO-PINCH was 100 A cm^{-2} , upon the cross-section of a single emitting filament. However, due to spacing considerations for closely packed emitting filaments, the maximum electrode plasma current density design for PROTO-SPHERA was further limited to $j_e \approx 80 \text{ A cm}^{-2}$. Therefore, at the plasma–cathode interface (which has the shape of a ribbon with radius $R_{EL} = 0.4$ m and vertical width $\Delta Z_{EL} \approx 3.0$ cm), the maximum total electrode plasma current was $I_e = 2\pi R_{EL} \Delta Z_{EL} j_e \approx 60$ kA.

2.2. The PF coils

A second constraint was the choice of reducing the versatility of the magnetic configuration by grouping the poloidal field (PF) coils surrounding the combined plasma into two sets, each composed of coils connected in series (see figure 3). The PF shaping coils, which have the task of shaping the SP, compose Group ‘B’; their current per turn $I_{B\cdot}$ remains fixed during the

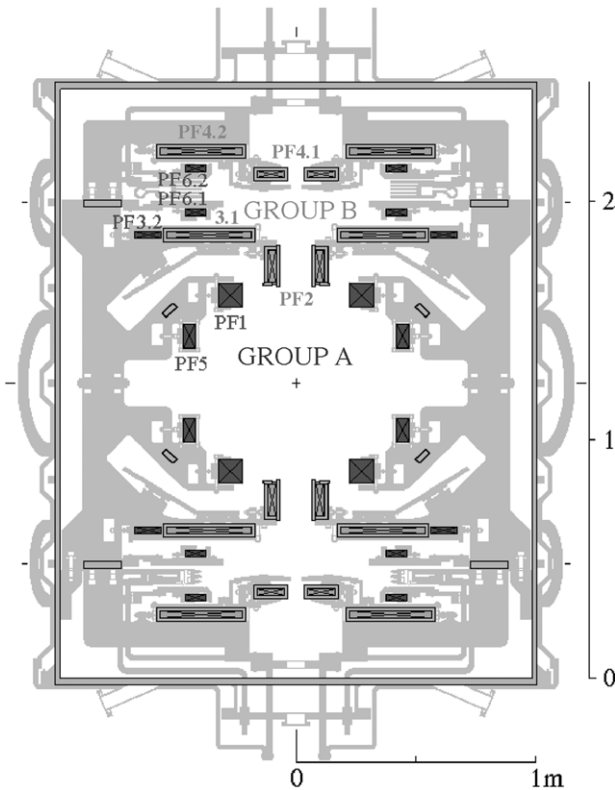


Figure 3. Poloidal field coils of PROTO-SPHERA, divided in groups 'A' (dark red) and 'B' (light green). All the axisymmetric passive conductors are also shown (light cyan).

plasma shot. The PF compression coils, which have the task of compressing the ST, compose Group 'A'; their current per turn I_A is variable during the plasma shot.

As the formation time of the ST is 1 ms, the coils whose variable currents compress the ST are shielded inside thin metal casings (time constant $\approx 200 \mu\text{s}$). On the other hand the coils whose constant currents shape the SP are enclosed inside thick metal casings (time constant $\geq 2 \text{ms}$), in order to stabilize the disc-shaped plasma near the electrodes during the formation of the ST.

A third constraint was in designing the PF coils large enough as to limit the current density flowing inside them. The last two are technical constraints, which serve the purpose of simplifying the design and of reducing the cost of a concept exploration experiment such as PROTO-SPHERA.

2.3. Outline of the operation

The START spherical tokamak [5] has been transferred to Frascati (May 2004) and disassembled (October 2004). The START cylindrical vacuum vessel (2.0 m in diameter), slightly extended in the vertical direction to 2.5 m, will contain the load-assembly of PROTO-SPHERA. The anode (top) will be at positive voltage, the PF coils can be floating and the cathode (bottom) will be at ground potential, together with the vessel and the remaining load-assembly. In the presence of a hot cathode the SP (guided by the Group 'B' PF shaping coils) will be formed at an electrode plasma current $I_e = 8.5 \text{kA}$, which guarantees MHD stability, as its MHD safety factor will be $q_{SP} > 2$. Note that for the PROTO-SPHERA configuration

q_{SP} is defined along the symmetry axis (poloidal turns/toroidal turns of a field line) and is therefore reversed with respect to q_{ST} defined along the ST magnetic axis (toroidal turns/poloidal turns of a field line).

In the PROTO-SPHERA experiment, raising the electrode plasma current up to $I_e = 60 \text{kA}$, the SP becomes unstable, as q_{SP} is much less than one. During the instability the Group 'A' PF compression coils will be switched on and the ST will be generated around the SP, driven in part by the inductive flux of the PF compression coils and in part by helicity injection from the SP. The formation sequence of PROTO-SPHERA will parallel the scheme successfully demonstrated by the TS-3 experiment at the University of Tokyo [7, 8], which in the early 1990s produced a small ST with $I_{ST} = 50 \text{kA}$ around a SP with $I_e = 40 \text{kA}$, for at least $80 \mu\text{s} \approx 100\tau_A$ (100 Alfvén times).

The first goal of the PROTO-SPHERA experiment is to compress the ST to the lowest possible aspect ratio ($A = 1.2-1.3$), in a time of about 1800 Alfvén times ($1800\tau_A \approx 1 \text{ms}$). The second goal is to show that efficient helicity injection can sustain the ST around the SP for at least one resistive time ($\tau_R \approx 70 \text{ms}$).

3. MULTI-PINCH as the first step of PROTO-SPHERA

MULTI-PINCH (see figure 4) is an initial experimental setup devoted to assess and clarify the most critical point of the PROTO-SPHERA experiment from the SP point of view: it explores the breakdown conditions and the pinch stability needed for the first phase of the PROTO-SPHERA discharge, in the presence of the Group 'B' PF shaping coils alone. In particular, in order to avoid the need of water-cooling, MULTI-PINCH produces a SP with reduced current ($I_e \leq 8.5 \text{kA}$, $q_{SP} \sim 2$) but with the same geometry and linear dimensions as the one of PROTO-SPHERA. Nevertheless, the four pairs of Group 'B' shaping PF coils become fully recovered for PROTO-SPHERA, since they are built ready for water-cooling.

In the Phase I operations of MULTI-PINCH a provisional linear hollow anode (similar to the one used on PROTO-PINCH [6]) is used, with hydrogen gas fluxed through its holes: therefore, the pinch is 'disc shaped' only in proximity to the annular cathode. The aim of this phase is to test the breakdown, without adding the complication of an annular anode. In Phase II the final PROTO-SPHERA annular anode is also inserted in MULTI-PINCH, in order to obtain the pinch breakdown in the exact PROTO-SPHERA geometry and in order to test the stability of the 'double disc-shaped' SP. The major concern is the possibility that the pinch discharge sticks on the anode surface in some specific toroidal position (arc-anchoring). The arc-anchoring was transiently observed in PROTO-PINCH only when the cathode filaments were heated by a DC current, but vanished after switching to AC current heating. The arc-anchoring in PROTO-PINCH transiently reduced the total arc current but did not push the local arc current density beyond its limit. Should a transient arc-anchoring happen, there is sufficient space left in MULTI-PINCH (and in PROTO-SPHERA) to allocate saddle coils that could turn around the arc-anchoring through a rotating magnetic field.

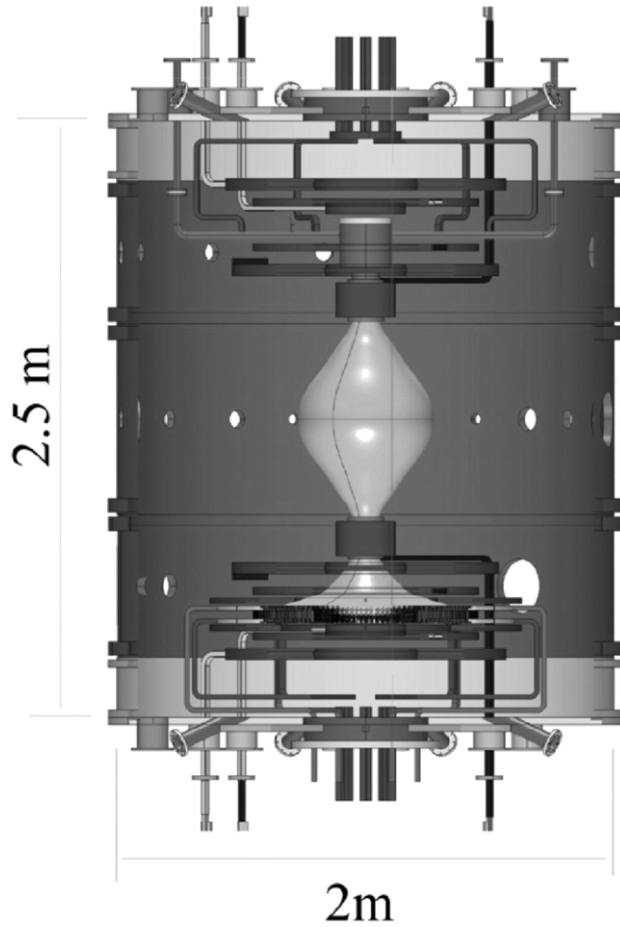


Figure 4. MULTI-PINCH (Phase I) assembled inside the START vacuum vessel. Note the presence of the Group ‘B’ PF shaping coils and the absence of the Group ‘A’ PF compression coils.

The MULTI-PINCH cathode will be the final PROTO-SPHERA cathode but only partially filled with tungsten filament modules (≤ 54 versus 378); each filament is exactly the same tested on PROTO-PINCH and will deliver its maximum electrode plasma current (150 A). It is the presence of a grounded hot cathode (the only electron emitter in the machine) that forbids any current path shorting the anode to the grounded vessel in PROTO-SPHERA (as it did in PROTO-PINCH): the anode current is really driven by the electrons emitted by the hot cathode.

4. Helicity injection in PROTO-SPHERA

4.1. Magnetic helicity injection

The Taylor assumption [9] states that the magnetic energy of a plasma decays to the minimum value it can have, subject to the conservation of magnetic helicity, which, for a simply connected volume, bounded by a magnetic surface, is defined as the gauge-invariant integral $K = \int \vec{A} \cdot \vec{B} dV$. Any initial plasma configuration, in the absence of external volume power sources, will self-organize in a relaxed state $\vec{\nabla} \wedge \vec{B} = \mu \vec{B}$, with a relaxation parameter $\mu = \mu_0 \vec{j} \cdot \vec{B} / B^2 = \text{constant}$ all over the plasma, after sufficient time.

A more realistic physical situation of a domain V_a containing a magnetized plasma, with open field lines passing through the boundary (whose outward pointing normal unit vector is \hat{n}_a), offers the opportunity of refurbishing the helicity content of the magnetized plasma. In this situation it is more suitable to define the relative magnetic helicity [10] $\Delta K = \int_{V_a} (\vec{A} + \vec{A}_V) \cdot (\vec{B} - \vec{B}_V) dV$, where the vacuum potential field $\vec{B}_V = \vec{\nabla} \wedge \vec{A}_V$ is determined in V_a by $\vec{\nabla} \wedge \vec{B}_V = 0$, with boundary conditions $\vec{B}_V \cdot \hat{n}_a = \vec{B} \cdot \hat{n}_a$. Plasma formation and sustainment can occur if the magnetic helicity can be injected through the boundary (by driving current along the lines of force) more quickly than it is dissipated inside the domain by resistive processes. The origin of magnetic helicity injection is connected with the electric current forced to flow along the magnetic field, generating perpendicular magnetic flux and causing the magnetic field lines to kink up, with a helical pattern. Magnetic flux, plasma current and magnetic energy are injected along with the magnetic helicity, and the reconnection processes convert part of the magnetic energy into kinetic energy of the magnetized plasma. If the helicity source (the SP discharge in the case of PROTO-SPHERA) is physically separated from the helicity sink (the ST of PROTO-SPHERA), a gradient in the relaxation parameter ($\vec{\nabla} \mu \neq 0$) appears: resistive MHD instabilities produce a helicity flow from regions of larger μ to regions of smaller μ . A diffusion coefficient or hyper-resistivity [11] was used as an ad hoc description of the helicity flux from source to sink.

4.2. Safety factor profile: comparison with TS-3 and Hill’s vortex

The literature has considered the equilibrium of a completely relaxed state, enclosed within a perfectly conducting portion of sphere, with radius R_{sph} , fed by two electrodes upon the polar caps:

- At the threshold, $\mu R_{\text{sph}} = 4.49$, the well-known classical spheromak solution [12] (Hill’s vortex) is obtained, with normal field component $\vec{B} \cdot \hat{n} = 0$ all over the sphere. However, the classical spheromak configuration, in the absence of a close fitting flux conserver, can be unstable to rotations and translations of the symmetry axis and is characterized by an MHD safety factor profile decreasing towards the edge ($q_{\text{axis}} \approx 0.8$, $q_{\text{edge}} \approx 0.7$).
- Beyond the threshold, $\mu R_{\text{sph}} > 4.49$, open flux current flows around the ST. The Taylor’s helicity injection theory [4] predicts that the configurations with $\mu R_{\text{sph}} > 4.49$ are ideal MHD unstable.
- Below the threshold, $\mu R_{\text{sph}} < 4.49$, a solution similar to PROTO-SPHERA is obtained. Open flux current flows from an anode on the top into a cathode on the bottom, through the hole of the ST (Taylor helicity drive).

The ideal stability threshold for PROTO-SPHERA (which will be described in section 7), being influenced by the absence of a conducting wall near the ST and by finite plasma pressure effects, can be far from the Hill’s vortex threshold. It is nevertheless worthwhile to compare the TS-3 experimental results with the design scenario for PROTO-SPHERA having the Hill’s vortex model as a background: this is done in figure 5. The idea of the PROTO-SPHERA experiment is to

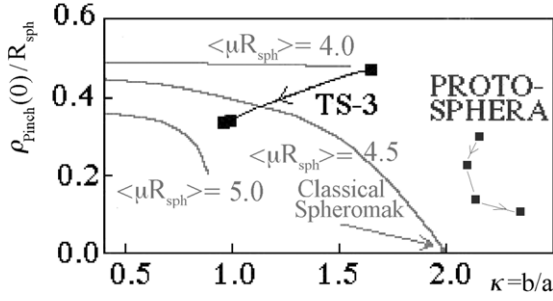


Figure 5. Formation and compression of PROTO-SPHERA, along with the values obtained in the TS-3 compression experiment, as a function of the ST elongation (κ) and the compression of the SP ($\rho_{\text{Pinch}}(0)/R_{\text{sph}}$). The values of $\langle \mu R_{\text{sph}} \rangle$ for the Hill's vortex model are used as a background, although the stability thresholds do not coincide with $\langle \mu R_{\text{sph}} \rangle = 4.49$ either for TS-3 or for PROTO-SPHERA.

drive the ST plasma, through a formation and compression scheme, towards a state not far from the stability threshold, while maintaining safety factor values inside it ($q_0 \approx 1$ at the magnetic axis; $q_{95} \approx 3$ at the surface that contains 95% of the poloidal flux included within the magnetic separatrix) typical of spherical tokamaks with metal centrepost. The aim is that of controlling the flow of the magnetic helicity towards the magnetic axis of the ST, while avoiding the complete relaxation of the system [13].

It is to be noted that the higher compression of the SP, ($\rho_{\text{Pinch}}(0)/R_{\text{sph}} \approx 0.10$) and the higher elongation of the ST ($\kappa \approx 2.3$), designed for PROTO-SPHERA with respect to TS-3, are the main tools for obtaining a high MHD safety factor inside the ST. Moreover, Farengo and Caputi [14] have employed the principle of minimum energy dissipation, with the constraint of helicity balance, for calculating the safety factor profile of PROTO-SPHERA. They have found that monotonically increasing q -profiles can be obtained if the resistivity is minimum at the ST magnetic axis; whether this assumption is compatible with sustainment through magnetic relaxation (for an equilibrium supported by PF coils and in the absence of a flux conserver near the plasma) remains an open question to be settled by the experiment.

4.3. Relaxation parameter profile and power transfer efficiency

The SPHEX experiment at UMIST (Manchester) has explored $\vec{\nabla} \mu$ in a FCS, created by a magnetized coaxial plasma gun. In agreement with the results of SPHEX [15], the PROTO-SPHERA equilibria, which will be presented in section 6, were calculated assuming that the ratio between the constant relaxation parameter μ_{SP} in the SP and the volume averaged $\langle \mu \rangle_{\text{ST}} = \mu_0 \langle \vec{j} \cdot \vec{B} / B^2 \rangle_{\text{ST}}$ in the ST is within the range $2.4 \leq \mu_{\text{SP}} / \langle \mu \rangle_{\text{ST}} \leq 3.3$. An ‘effective loop voltage’ can be defined as the one required to get the same helicity injection through ohmic heating: $V_{\text{loop}} \leq V_{\text{inj}}(\psi_{\text{inj}} / \Psi_{\text{ST}})$, where the equality sign means perfect helicity transfer, Ψ_{ST} is the toroidal flux within the ST, ψ_{inj} the poloidal flux within the injector (SP) and $V_{\text{inj}} = V_e$ the total voltage drop between the electrodes. For the Taylor helicity drive of PROTO-SPHERA the injector and the separatrix poloidal flux coincide, $\psi_{\text{inj}} = \psi_X$, as well as the injector and the electrode plasma current, $I_{\text{inj}} = I_e$. Therefore,

the ‘power transfer efficiency’ is $\varepsilon = I_{\text{ST}} V_{\text{loop}} / I_{\text{inj}} V_{\text{inj}} \leq I_{\text{ST}} \psi_X / I_e \psi_{\text{ST}} = \langle \mu \rangle_{\text{ST}} / \mu_{\text{inj}}$. Experimental results for the spherical tokamak HIT [16], sustained by helicity injection showed that only 25% of the total injected power was not dissipated within the injector itself and that furthermore only 25% of that power went into the spherical tokamak current drive; therefore, $\varepsilon \approx 0.12 \cdot \langle \mu \rangle_{\text{ST}} / \mu_{\text{inj}}$, with $\langle \mu \rangle_{\text{ST}} / \mu_{\text{inj}} \approx 0.5$. More recent results [17] for sustained high temperature ($T_{e0} \approx 110$ eV) discharges of SSPX give $\varepsilon \approx 0.10 \cdot \langle \mu \rangle_{\text{ST}} / \mu_{\text{inj}}$, with $\langle \mu \rangle_{\text{ST}} / \mu_{\text{inj}} \approx 0.5$ –1, and moreover it is found that the sheaths voltage drop (~ 100 V) accounts for 70–80% of the total voltage drop between the electrodes. In agreement with the results of SSPX the power transfer efficiency for the helicity injection sustainment of PROTO-SPHERA will be estimated in section 6 as

$$\varepsilon = I_{\text{ST}} V_{\text{loop}} / I_e V_e = 0.10 \cdot \langle \mu \rangle_{\text{ST}} / \mu_{\text{SP}}. \quad (1)$$

5. The predictive equilibrium code for PROTO-SPHERA

5.1. Assumptions

A reconstructive MHD equilibrium code based upon spherical multipolar expansion has already been presented [18], so only a few necessary details about its predictive version will be added in this paper. The main advantages of multipolar MHD equilibrium solvers with respect to finite element method MHD equilibrium solvers are the speed of the computations, due to the analytical basis functions, and the ease in introducing changes into the configuration, due to the geometrically fixed numerical mesh. The disadvantage is a larger inaccuracy in the solution, due to the multipolar truncation, a problem that does not exist in finite element method MHD equilibrium solvers [19,20], where careful placements of the finite elements can allow for greater numerical accuracy.

In the case of PROTO-SPHERA the plasma–electrode contact surfaces are cylindrical ribbons with radius $R_{\text{EL}} = 0.4$ m and vertical width $\Delta Z_{\text{EL}} \approx 3.0$ cm (see figure 1). Free-boundary equilibrium calculations, based on the poloidal flux $\psi = \int \vec{B} \cdot d\vec{S}_p = 2\pi R A_\phi$ contained inside each magnetic surface (where R is the distance from the symmetry axis and A_ϕ is the toroidal component of the vector potential), have been performed. The Grad–Shafranov equation

$$\begin{aligned} \frac{\partial^2 \psi}{\partial R^2} + \frac{\partial^2 \psi}{\partial Z^2} - \frac{1}{R} \frac{\partial \psi}{\partial R} \\ = -4\pi^2 \mu_0 R^2 \frac{dP(\psi)}{d\psi} - 4\pi^2 f(\psi) \frac{df(\psi)}{d\psi} \\ = -2\pi \mu_0 R j_\phi \end{aligned} \quad (2)$$

is solved under the following assumptions.

- (i) The SP is a homogeneous force-free ($\vec{\nabla} p = 0$, $\vec{\nabla} \mu = 0$) plasma. Therefore [21];

$$\begin{aligned} p(\psi) = p_{\text{edge}} = \text{const} \\ \text{and } f(\psi) = (\mu_0 I_e / 2\pi)(\psi / \psi_X) \end{aligned} \quad (3)$$

inside the SP ($0 < \psi < \psi_X$), with $\psi = 0$ on the symmetry axis and $\psi = \psi_X$ at the embedded magnetic separatrix. The total electrode plasma current I_e as well as the kinetic pressure p_{edge} inside the SP are inputs.

- (ii) The ST–SP interface is defined by the embedded separatrix (with non-orthogonal crossing of the separatrix tails, due to the presence of non-vanishing toroidal plasma current density $j_\varphi \neq 0$ upon the regular X-points). The plasma current density is non-vanishing ($\vec{j} \neq 0$), within the volume bounded by the separatrix for the ST and within the volume limited by the electrodes for the SP (see figure 6).
- (iii) The kinetic plasma pressure $p(\psi)$ and the normalized poloidal plasma current $f(\psi) = (1/2\pi) \int \vec{\nabla} \wedge \vec{B} \cdot d\vec{S}_p = \mu_0 I_{\text{dia}}(\psi)/2\pi = RB_\varphi$ (where B_φ is the toroidal component of the magnetic field and I_{dia} the poloidal plasma current) are continuous at the ST–SP interface ($\psi = \psi_X$), whereas the total plasma current density \vec{j} may have jumps at the ST–SP interface.
- (iv) Inside the ST ($\psi_X < \psi \leq \psi_{\text{max}}$, where ψ_{max} is the poloidal flux at the magnetic axis)

$$p(\psi) = p_{\text{edge}} + C_p(\psi - \psi_X)^{1.1}$$

and

$$f^2(\psi) = (\mu_0 I_e/2\pi)^2 + C_f(\psi - \psi_X)^{1.1}. \quad (4)$$

- (v) The total toroidal plasma current flowing inside the ST, I_{ST} , is an input, along with the total poloidal plasma beta inside the volume of the ST:

$$\beta_p^{\text{ST}} = \frac{2}{\mu_0 (I_{\text{ST}})^2} \left(\int_{V_{\text{ST}}} \frac{p dV}{V_{\text{ST}}} \right) \left(\oint_{C^{\text{ST}}(\psi_X)} \hat{e}_p \cdot d\vec{l}_p \right)^2, \quad (5)$$

where \hat{e}_p is the poloidal unit vector and $d\vec{l}_p$ is the differential poloidal arc-length along the contour $C^{\text{ST}}(\psi_X)$ of the ST cross-section. The total toroidal plasma current I_φ^{SP} inside the SP is instead a result of the calculation.

- (vi) The inputs I_e and p_{edge} , along with I_{ST} and β_p^{ST} , determine, by an iterative solution, the values of C_p and C_f in (4), as well as the position and the value of the poloidal flux ($\psi = \psi_X$) at the embedded magnetic separatrix.
- (vii) The external equilibrium currents have been chosen according to the constraints of the PROTO-SPHERA experiment, illustrated in section 2, whereby the PF coils are grouped in two sets, each composed of coils connected in series (see figure 3).

5.2. Results

The iterative equilibrium calculation is performed in spherical coordinates (r, ϑ, φ) , where the poloidal flux can be expanded, in terms of index-1 order- n axisymmetric spherical harmonics $\sin \vartheta P_n^1(\cos \vartheta)$ and of the internal $M_n^i(r)$ and external $M_n^e(r)$ spherical multipolar moments, as

$$\psi = \sum_{n=1}^{N_{\text{max}}} [M_n^i(r)r^{-n} + M_n^e(r)r^{n+1}] \sin \vartheta P_n^1(\cos \vartheta). \quad (6)$$

It is necessary to resort to a large number of spherical harmonics ($N_{\text{max}} = 40\text{--}50$) in order to obtain a correct description of the SP.

The highest value of the safety factor of the lines of force that can be calculated at the edge of the ST is $q_\psi \approx 6$, for $|\psi - \psi_X| \approx 10^{-3}\psi_{\text{max}}$. The rather high values of $q_0 \approx 0.94$, at the magnetic axis, and of $q_{\text{min}} \approx 0.88$, at an intermediate

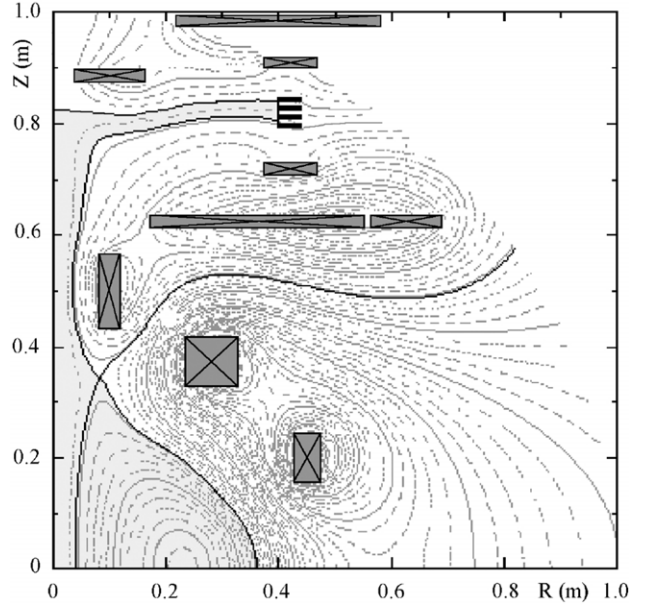


Figure 6. Equilibrium calculation for PROTO-SPHERA: $I_{\text{ST}} = 180$ kA, $I_e = 60$ kA, $\beta_p^{\text{ST}} = 0.22$. Contour plot of the poloidal flux ψ . The domains where plasma current density flows are grey-filled.

radius, are due to very strong toroidal paramagnetism, which pushes the total toroidal magnetic field B_φ at the position of the magnetic axis well beyond the value $B_{\varphi 0}$ due to the electrode plasma current I_e alone, $B_\varphi(R_{\text{axis}})/B_{\varphi 0}(R_{\text{axis}}) > 1$. However, the region of strong shear at the edge starts at $q_{95} \approx 2.6$ (surface which contains 95% of the poloidal flux included within the magnetic separatrix) and is extremely narrow, as shown in figure 7. The flux surface averaged [22] relaxation parameter $\langle \mu \rangle = \mu_0 \langle \vec{j} \cdot \vec{B} / B^2 \rangle$ is constant ($\mu \rangle = \mu_{\text{SP}} \approx 35 \text{ m}^{-1}$ inside the force-free SP; $\langle \mu \rangle$ decreases to a value around 9 m^{-1} near the ST magnetic axis. Inside the ST the volume-averaged value $\langle \mu R_{\text{sph}} \rangle_{\text{ST}}$ is about 4.

Different profiles for $p(\psi)$ and $f(\psi)$, explored in the appendix as apparently better suited to helicity injected equilibria, have much less shear near the edge. It is obvious that transport studies and detailed helicity injection models, not addressed in this paper, should be included to accurately predict the shape of the profiles.

6. Equilibrium formation and compression sequence for PROTO-SPHERA

6.1. Breakdown and sustainment of the stable SP

The force-free SP is formed by a hot cathode breakdown, following the method developed in PROTO-PINCH [6]. First, the cathode tungsten filaments are heated to 2600°C in about 20 s, while the current in the PF-shaping coils of Group ‘B’ reaches its constant value $I_{\text{B}} = 1875$ A in less than 1 s (figure 8). Then a fast gas valve puffs Hydrogen through the hollow anode in order to fill the SP discharge region at a pressure $p_{\text{H}} \approx 10^{-3}\text{--}10^{-2}$ mbar. Within less than 2 ms a total voltage $V_e \approx 100\text{--}200$ V is applied between the anode and the cathode, in order to obtain the SP breakdown. The SP ohmic dissipation, P_e^{oh} , and the electron temperature in the

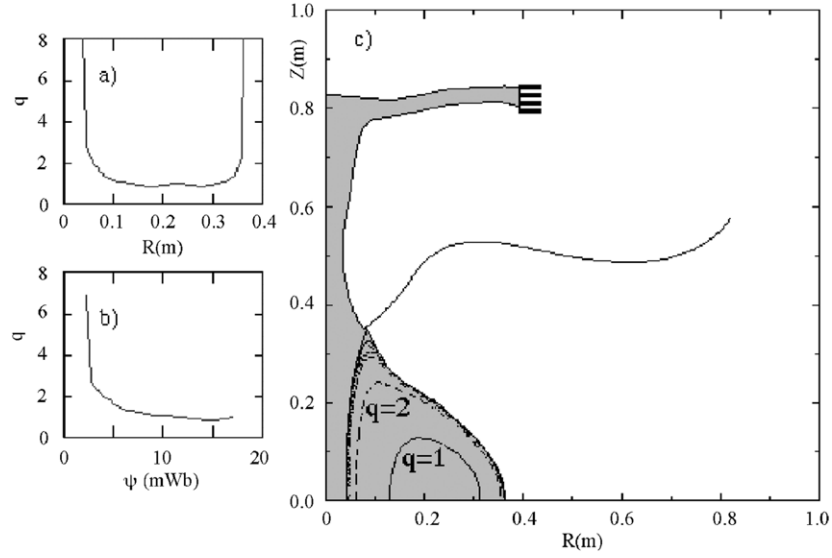


Figure 7. Equilibrium calculation for PROTO-SPHERA: $I_{ST} = 180$ kA, $I_e = 60$ kA, $\beta_p^{ST} = 0.22$. (a) MHD safety factor q on the midplane. (b) q inside the ST as a function of the poloidal flux ψ . (c) Contour plot of the integer values of q .

main body of the SP, T_e^{Pinch} , are predicted [2] by equating, far from the electrodes along the open flux surfaces, the current convective loss to the ohmic input:

$$\frac{5}{2} T_e^{\text{Pinch}} I_e = \frac{2I_e^2 L_{\text{Pinch}} Z_{\text{eff}} / \pi \rho_{\text{Pinch}}^2(0)}{5 \cdot 10^2 \ln \Lambda (T_e^{\text{Pinch}})^{3/2}}, \quad (7)$$

where P_e^{oh} is modelled for a straight cylinder with electrode connection length $2L_{\text{Pinch}} = 4$ m and Z -averaged pinch cross-section $\langle 1/\rho_{\text{Pinch}}^2(Z) \rangle = 1/(2.5 \cdot \rho_{\text{Pinch}}^2(0))$, with $\rho_{\text{Pinch}}(0) = 0.277$ m. With $I_e = 8.5$ kA, $Z_{\text{eff}} = 2$ and Coulomb logarithm $\ln \Lambda = 8$, this calculation gives $T_e^{\text{Pinch}} = 3.8$ eV and an ohmic input power $P_e^{\text{oh}} = 80$ kW. Assuming that in PROTO-SPHERA the electrode plasma parameters will be the same as in the PROTO-PINCH electrode's testbench [6], the electrode voltage sheath drop is predicted to be $V_e^{\text{sheath}} = 77$ V, yielding $P_e^{\text{sheath}} = V_e^{\text{sheath}} \cdot I_e \leq 0.65$ MW.

At the maximum pressure $p_H \approx 10^{-2}$ mbar, with an SP discharge volume of 0.25 m³, requiring 20 eV for ionization and heating the discharge at $T_e^{\text{Pinch}} = 3.8$ eV and assuming 25% efficiency in the process, about 1.7 kJ of energy is needed. Given the inductance of the arc discharge $L_{\text{Pinch}} = 0.8$ μ H a further 0.3 kJ is needed for the magnetic energy. At the maximum voltage of the anode feeder (350 V), the power provided is 1.5 kJ ms⁻¹, during the I_e current start-up. This means that the arc current can be raised to 8.5 kA in a few milliseconds. The electrode plasma current is then limited to $I_e \leq 8.5$ kA (figure 8), while the total toroidal current inside the force-free SP is $I_\phi^{\text{SP}} \approx 3$ kA, as calculated by the equilibrium solver. The SP discharge (see figure 9) is kink stable ($q_{\text{SP}} \geq 2$, $\mu_{\text{SP}} \approx 2.6$ m⁻¹). No current flows in the PF compression coils of Group 'A': this is exactly the configuration described in section 3, which will be tested in Phase II of the MULTI-PINCH experimental setup.

As the power required to maintain the kink-stable SP will be quite low (<1 MW), this discharge can be easily sustained for 1 s. In the scenario shown in figure 8 the stable SP is maintained for only 0.1 s. During this time interval it should be possible to increase or decrease the SP electron density, puffing

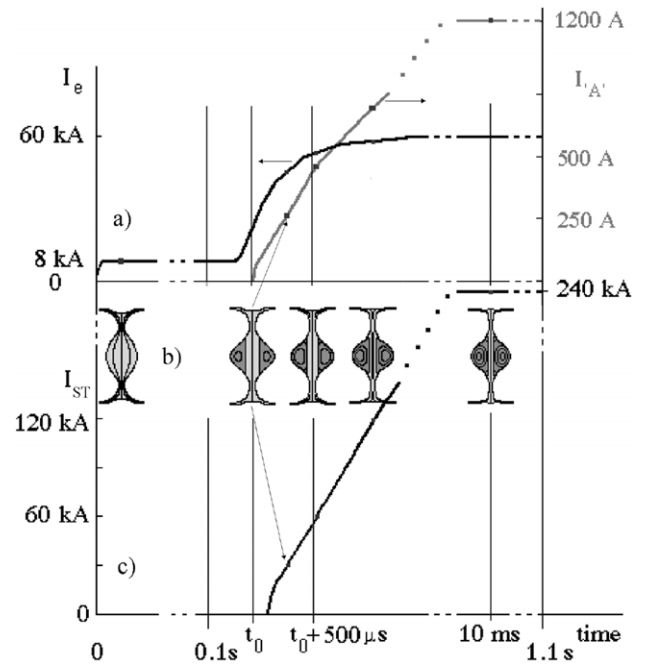


Figure 8. Formation and compression time sequence: (a) waveforms of the electrode plasma current (I_e) and of the current in the compression PF coils ($I_{A'}$); (b) sketch of the plasma poloidal cross-sections and (c) waveform of the toroidal current in the ST (I_{ST}).

with the fast gas valve through the hollow anode. This control tool would be quite useful should the best choice for the gas pressure at the SP breakdown turn out to be incompatible with the best choice for the electron density at the ST formation.

6.2. Start-up and ramp-up of the ST

Pushing the electrode plasma current up to $I_e = 60$ kA ($\mu_{\text{SP}} \approx 18$ m⁻¹), on a time scale of about 500 μ s (figure 8(a)), the SP goes kink unstable ($q_{\text{SP}} < 2$). With a delay of about 100 μ s

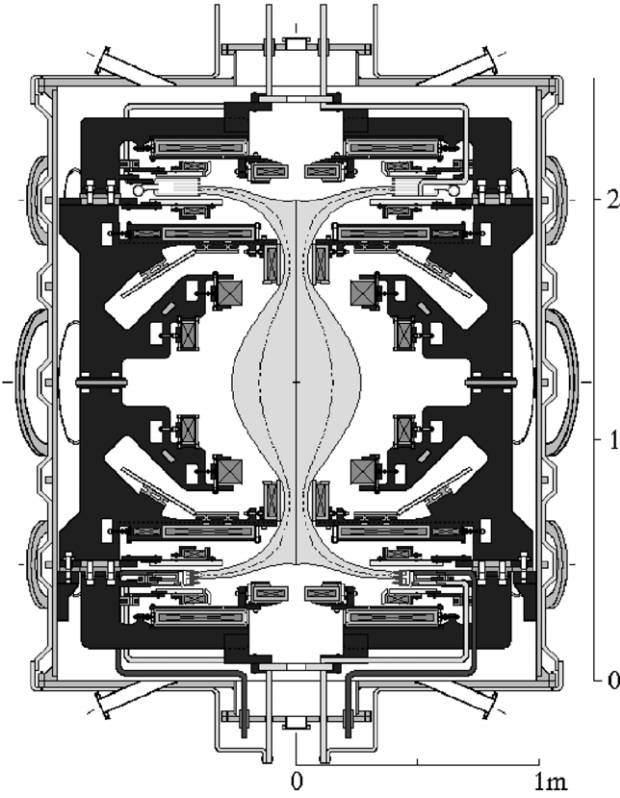


Figure 9. Equilibrium of PROTO-SPHERA at the formation of the SP, with plasma electrode current $I_e = 8.5$ kA.

also the current in the PF compression coils of Group ‘A’ starts to increase, reaching $I_{A'} \approx 0.7$ kA on a time scale of ≈ 1 ms (figure 8(a)). After a further delay of $100 \mu\text{s}$ the ST is formed, as in the TS-3 experiment [7], compressed (figure 8(b)) and reaches $I_{ST} = 120$ kA on a time scale of ≈ 1 ms (figure 8(c)). The success of the TS-3 formation scheme could have been due in part to the flux swing induced by the increase in the current in the PF compression coils. As a matter of fact, the PF compression coils flux swing available in PROTO-SPHERA provides a loop voltage $V_{\text{loop}} = 10$ V, for about 1 ms. This flux swing alone should be able to push I_{ST} up to 120 kA in about 1 ms, which is a figure easily achieved in spherical tokamak start-up in the absence of central solenoid flux [5].

Assuming $I_e = 60$ kA, $Z_{\text{eff}} = 2$ and Coulomb logarithm $\ln \Lambda = 10$, the calculation (4) gives an increase from $P_e^{\text{oh}} = 2.4$ MW, $T_e^{\text{Pinch}} = 16$ eV (at $I_{ST} = 30$ kA and $\rho_{\text{Pinch}}(0) = 0.11$ m) up to $P_e^{\text{oh}} = 5.4$ MW, $T_e^{\text{Pinch}} = 36$ eV (at $I_{ST} = 180$ kA and $\rho_{\text{Pinch}}(0) = 0.04$ m), corresponding to $40 \text{ V} \leq V_e^{\text{oh}} \leq 90$ V. On the other hand, the dissipation at the electrode sheaths scales linearly with I_e and then maintains the constant value $P_e^{\text{sheath}} = V_e^{\text{sheath}} \cdot I_e \leq 4.6$ MW during the toroidal plasma sustainment at $I_e = 60$ kA. Given the inductance of the arc, the ramp-up of I_e requires an additional inductive electrode voltage drop V_e^L , which decreases from $V_e^L = 100$ V, well before the formation of the toroidal plasma, down to $V_e^L = 50$ V at the formation of the toroidal plasma and finally vanishes when $I_{ST} = 120$ kA is reached (see figure 8(a)). Putting together all the dissipative and inductive effects on the SP plasma, the required electrode voltage drop decreases from $V_e = 220 \text{ V} + V_e^{\text{HI}}$ down to $V_e = 170 \text{ V} + V_e^{\text{HI}}$

during the formation of the toroidal plasma, the additional term V_e^{HI} being the electrode voltage drop due to helicity injection. Balancing the electron pressure in the main body of the SP with that at the electrodes, and assuming that in PROTO-SPHERA the electrode plasma parameters will be the same as in the PROTO-PINCH electrode’s testbench [6] ($T_e^{\text{sheath}} = 0.5$ eV, $n_e^{\text{sheath}} = 5 \cdot 10^{20} \text{ m}^{-3}$), the electron density of the main body of the SP should be about $n_e^{\text{Pinch}} = 1.5 \cdot 10^{19} \text{ m}^{-3}$. High-Z materials compose all the machine load assembly inside the vacuum vessel, and a baking system effective for removing water vapour is used [2]. The power lost through impurity radiation is calculated assuming a 1% impurity concentration and a cooling rate $R(T_e) \approx 10^{-31} \text{ Wm}^3$, which corresponds to the maximum cooling rate of oxygen. The resulting low-Z impurity power loss from the SP is $P_e^{\text{rad}} \approx 0.1$ MW, which is negligible.

At the maximum pressure $p_H \approx 10^{-2}$ mbar, with an ST+SP discharge volume of 0.25 m^3 , requiring 40 eV for heating the plasma and assuming 25% efficiency in the process, about 3.3 kJ of energy is needed. Given the inductances of the arc discharge and of the ST, further 0.8 kJ and 1.1 kJ must be added, respectively, for the ST and the SP magnetic energy, giving a total energy requirement of 5.2 kJ during the I_e current ramp-up. At the maximum voltage of the anode feeder (350 V), the provided power is 10.5 kJ ms^{-1} , whereas at the maximum voltage of PF ‘A’ feeder (16 kV), a further power of 5.5 kJ ms^{-1} is provided, giving a total available power of 16 kJ ms^{-1} . This means that the ramp-up of I_{ST} to 120 kA in about 1 ms is feasible.

6.3. Modelling of the ST

In order to design the formation and compression sequence, the performances of the closed flux surfaces ST plasma have been modelled under the following assumptions.

- The total energy confinement time inside the ST is evaluated from the semi-empirical Lackner–Gottardi L-mode plateau scaling [23].
- The total helicity injection power required to sustain the ST (1) is taken as $p_{\text{HI}}^{\text{ST}} = 0.10 \cdot I_e V_e(\mu)_{\text{ST}} / \mu_{\text{SP}}$; therefore, $P = P_{\text{HI}}^{\text{ST}}$ is used in the confinement scaling and $V_e^{\text{HI}} = 0.10 \cdot V_e(\mu)_{\text{ST}} / \mu_{\text{SP}}$ is the electrode voltage drop due to helicity injection.
- The electron density is taken as the one corresponding to the maximum volume averaged electron density $\langle n_e \rangle_{\text{ST}}$ that makes the ideal MHD β limit compatible (which will be given in detail in section 7) with the Lackner–Gottardi L-mode plateau scaling; $\langle n_e \rangle_{\text{ST}}$ turns out to be much smaller than the Greenwald density limit [24].

These assumptions give, with $I_{ST} = 180$ kA, $Z_{\text{eff}} = 2$ and a volume-averaged electron density $\langle n_e \rangle_{\text{ST}} = 5.0 \cdot 10^{19} \text{ m}^{-3}$, a volume-averaged electron temperature $\langle T_e \rangle_{\text{ST}} = 140$ eV and an input power $p_{\text{HI}}^{\text{ST}} = 300$ kW, corresponding to $V_e^{\text{HI}} = 5$ V and therefore to a total electrode voltage drop $V_e = V_e^{\text{sheath}} + V_e^{\text{oh}} + V_e^{\text{HI}} \approx 170$ V. Repeating the calculation, under the same assumptions but with different levels of I_{ST} , one obtains the result that the formation and compression sequence should develop at roughly constant (volume averaged) plasma-beta value in the ST:

$$\beta_{\text{ST}} = 2\mu_0 \langle p \rangle_{\text{ST}} / \langle B^2 \rangle_{\text{ST}} \approx 0.15\text{--}0.2. \quad (8)$$

6.4. Time scale and formation sequence

The Alfvén time is calculated as $\tau_A \approx 0.55 \mu\text{s}$; the resistive time is calculated as $\tau_R \approx 70 \text{ ms}$; therefore, the magnetic Lundquist number of PROTO-SPHERA should be $S = \tau_R/\tau_A \approx 1.2 \cdot 10^5$; a similar estimate for the data of TS-3 flux-core experiment gives $S = \tau_R/\tau_A \approx 9 \cdot 10^3$. Magnetic reconnections are required to form the ST from the SP, if the current ramp-up is dominated by the helicity injection from the unstable SP. Therefore, the time required for the formation of PROTO-SPHERA must be extrapolated from the experimental results of the TS-3 flux-core spheromak using the reconnection time scale. The Sweet–Parker reconnection theory [25, 26] predicts that the reconnection time scales like $S^{1/2}\tau_A$. TS-3 requires $80 \mu\text{s}$ to reach [8] a ratio $I_{ST}/I_e = 50 \text{ kA}/40 \text{ kA}$. The time scale for the formation of PROTO-SPHERA is estimated to be $210 \mu\text{s}$, in order to reach the same current ratio $I_{ST}/I_e = 75 \text{ kA}/60 \text{ kA}$. As a consequence, a minimum time scale of $350 \mu\text{s}$ is required in order to reach $I_{ST} = 120 \text{ kA}$. Furthermore, accounting for the inductive flux delivered by the PF compression coils, the time evolution of the eddy current distribution over all the axisymmetric passive conductors inside the machine vacuum vessel (see figure 5) was calculated [2] to introduce a further $650 \mu\text{s}$ delay: therefore, a total time scale of 1 ms is required for achieving $I_{ST} = 120 \text{ kA}$.

The formation sequence starts $250 \mu\text{s}$ after the torus formation with $I_{ST} = I_e/2 = 30 \text{ kA}$: the equilibrium (figure 10(a)) has an aspect ratio $A = 1.80$, an elongation $\kappa = 2.17$, a limited paramagnetic effect $B_\varphi(R_{\text{axis}})/B_{\varphi 0}(R_{\text{axis}}) = 1.20$, a toroidal pinch current $I_\varphi^{\text{SP}} = 179 \text{ kA}$ and a safety factor profile with $q_0 = 1.2$, $q_{95} = 3.4$. The relaxation parameter in the pinch is $\mu_{\text{SP}}R_{\text{sph}} = 6$ and its volume average inside the ST $\langle \mu R_{\text{sph}} \rangle_{\text{ST}} \approx 2.5$ (with $R_{\text{sph}} = 0.35 \text{ m}$). The formation sequence continues $500 \mu\text{s}$ after the torus formation with $I_{ST} = I_e = 60 \text{ kA}$: the equilibrium has an aspect ratio $A = 1.51$, an elongation $\kappa = 2.15$, a relevant paramagnetic effect $B_\varphi(R_{\text{axis}})/B_{\varphi 0}(R_{\text{axis}}) = 1.47$, a toroidal pinch current $I_\varphi^{\text{SP}} = 247 \text{ kA}$ and a safety factor profile with $q_0 = 1.1$, $q_{95} = 2.9$. The relaxation parameter in the pinch is $\mu_{\text{SP}}R_{\text{sph}} = 8$ and its volume average inside the ST $\langle \mu R_{\text{sph}} \rangle_{\text{ST}} \approx 3.1$.

The formation sequence continues $1000 \mu\text{s}$ after the torus formation with $I_{ST} = 2I_e = 120 \text{ kA}$: the equilibrium has an aspect ratio $A = 1.32$, an elongation $\kappa = 2.16$, a large paramagnetic effect $B_\varphi(R_{\text{axis}})/B_{\varphi 0}(R_{\text{axis}}) = 2.1$, a toroidal pinch current $I_\varphi^{\text{SP}} = 310 \text{ kA}$ and a safety factor profile with $q_0 = 1.0$, $q_{95} = 2.8$. The relaxation parameter in the pinch is $\mu_{\text{SP}}R_{\text{sph}} = 10.5$ and its volume average inside the ST $\langle \mu R_{\text{sph}} \rangle_{\text{ST}} \approx 3.8$. After this time-slice the flux swing available from the PF compression coils is almost completely exhausted and any further increase in the ST total toroidal current relies upon efficient helicity injection. The time scale for reaching the full current, $I_{ST} = 4I_e = 240 \text{ kA}$, is estimated to be about 10 ms (which is shorter than the resistive time) from the results of helicity increase experiments in SSPX [17] and from the calculation of spheromak formation from instability saturation [27]: the equilibrium has an aspect ratio $A = 1.21$, an elongation $\kappa = 2.35$, a huge paramagnetic effect $B_\varphi(R_{\text{axis}})/B_{\varphi 0}(R_{\text{axis}}) = 3.1$, a toroidal pinch current $I_\varphi^{\text{SP}} = 407 \text{ kA}$ and a safety factor profile with $q_0 = 1.0$, $q_{95} = 2.7$. The relaxation parameter in the pinch is $\mu_{\text{SP}}R_{\text{sph}} = 14$ and its volume average inside the ST $\langle \mu R_{\text{sph}} \rangle_{\text{ST}} \approx 4.2$. The

equilibrium is shown in figure 10(b). It is possible that, after 10 ms, during the sustainment by helicity injection, the MHD activity does not settle into steady state but exhibits intermittent relaxations with toroidal number $n = 1$ (or with other low n numbers), with a period [27] shorter than the resistive time scale (70 ms). This would make the notion of axisymmetric equilibrium somewhat invalid during helicity driven operation.

It is to be noted that the equilibrium magnetic configuration proposed for the PROTO-SPHERA experiment is quite robust. Even without adding new power supplies, the PF compression coils belonging to Group ‘A’ are able to handle almost any changes in the internal plasma profiles, preserving both the SP shape near the electrodes as well as the spherical-tokamak-like safety factor profile in the ST ($q_{95} \approx 3$, $q_0 \geq 1$), even during the formation and compression phase. Therefore, the current of the compression PF coils I_{A} can be pre-programmed during the plasma current start-up and ramp-up and then feedback-controlled during the flattop. A more detailed analysis about the resilience of the PROTO-SPHERA equilibria is presented in the appendix.

7. Results of the ideal MHD stability analysis

7.1. Stability against loss of plasma configuration

As finite amplitude resistive MHD instabilities are required to produce the helicity flow from the SP to the ST, the combined PROTO-SPHERA configuration should be near the ideal MHD stability boundary in order to provide an intermittent mode with $n = 1$ [15] (or with other low n numbers). However, modes that would lead to loss of plasma configuration must be stable during operation: the simplest are the rigid vertical shift and the rigid tilt displacements. The result of their analysis is that the metal casings of the shaping PF coils are sufficiently thick as to stabilize the rigid vertical displacement of the ST during the formation phase. A further result is that the external field, produced by the PF coils, is such as to stabilize the rigid tilt displacement of the ST during the formation phase. The magnetic dipole moment of PF2 and PF3 divertor coils (see figure 3) provides the larger part of the plasma disc-shaping field near the electrodes. It can stabilize the rigid tilt instability, as it is aligned with the ST magnetic dipole moment and dominates over the opposite (destabilizing) dipole moment of PF1, PF5 and PF4.

7.2. Ideal MHD stability for low toroidal mode number

The more general issue of the ideal MHD stability of PROTO-SPHERA with respect to modes with low toroidal mode number ($n = 0-3$) has led to the development of a new finite element method stability code [20, 28] that will be fully presented in forthcoming papers, together with its results. Nevertheless, the ideal MHD stability results for PROTO-SPHERA can be summarized in the following way.

- The most relevant parameter appears to be the current ratio I_{ST}/I_e .
- The PROTO-SPHERA ST plasma-beta limit goes from $\beta_{\text{ST}} \sim 25\%$ to 30% at $I_{ST}/I_e \leq 1$ down to $\beta_{\text{ST}} \sim 14-16\%$ for $I_{ST}/I_e = 4$, with small variations due to the internal profiles. It is to be noted that if the ST vacuum toroidal beta

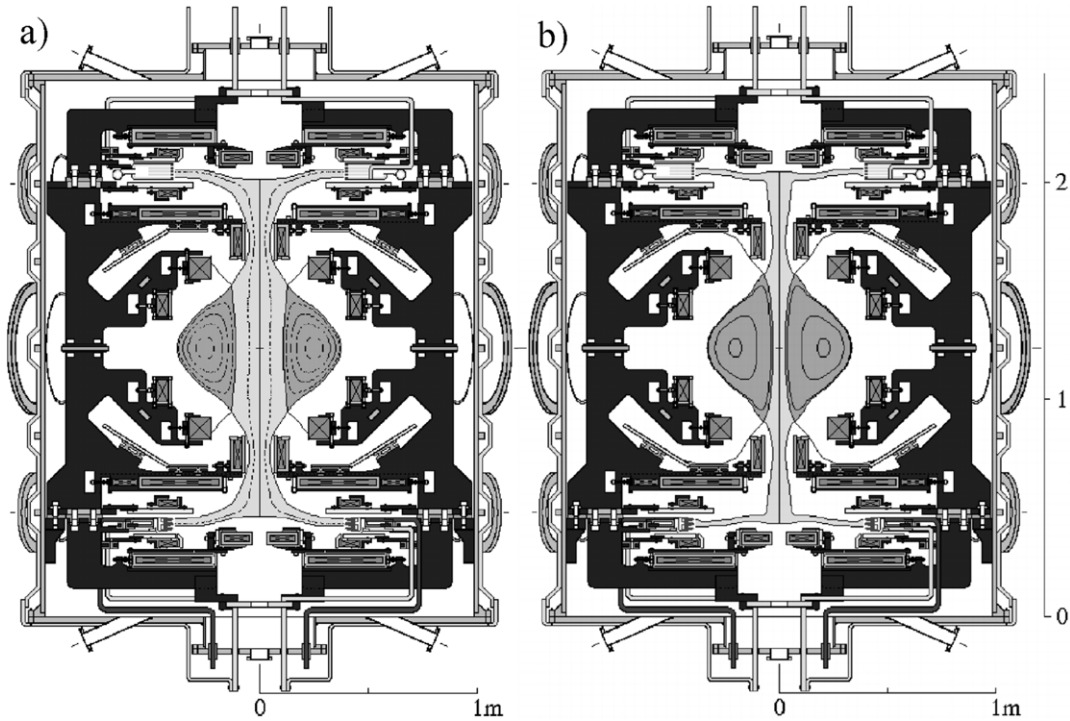


Figure 10. Equilibria of PROTO-SPHERA with plasma electrode current $I_e = 60$ kA: (a) $I_{ST} = 30$ kA, 250 μ s after ST formation and (b) $I_{ST} = 240$ kA, 10 ms after ST formation.

$\beta_{T0} = 2\mu_0 \langle p \rangle_{ST} / \langle B_{T0}^2 \rangle_{ST}$ were to be used (where B_{T0} is the toroidal field generated by the longitudinal current I_e flowing between the electrodes) the PROTO-SPHERA beta limit would correspond to $\beta_{T0} = 25\text{--}30\%$ for $I_{ST}/I_e = 0.5$ and to $\beta_{T0} = 72\text{--}84\%$ for $I_{ST}/I_e = 4$.

- Pressure-driven ideal MHD instabilities can appear inside the ST for $I_{ST}/I_e < 3$ (see figure 11(a)).
- Beyond this level of I_{ST}/I_e , the driving term becomes the kink of the SP, which on its turn causes the tilt of the ST (see figure 11(b)). In this latter case a too-strong instability of the SP could show up as an anode arc-anchoring, which is expected to reduce the available arc current I_e : the onset of such a limit upon I_e would imply a very hard limit upon I_p .

8. Conclusions

The PROTO-SPHERA configuration is a FCS with the Taylor helicity drive [4] configuration, i.e. with the open flux current (SP) passing through the hole of the ST, from the injector anode on the top of the plasma into the cathode on the bottom. The idea is that this helicity drive may be less disruptive than the conventional geometry of a FCS formed by a coaxial plasma gun, where the current returns around the outside of the plasma but with an uncontrollable path, which implies field errors. Another feature is that, whereas FCS formation through magnetized plasma guns requires breakdown in small spaces, with high filling pressures and kilovolt voltages, PROTO-SPHERA will instead form at spherical-tokamak-like densities, with low voltage drop (≈ 200 V) between electrodes and will not undergo any expansion or acceleration. The advantage of this formation scheme may be that of avoiding

the release of large amounts of neutrals and impurities and the amplification of field errors by large-scale plasma motion.

From the MHD equilibrium point of view PROTO-SPHERA is formed in the absence of a nearby closed conducting shell by pulsing the compression PF coils, following the scheme pioneered by the TS-3 compression experiment [8]: the flux swing due to this pulsing alone should be able to push I_{ST} up to 120 kA in about 1 ms. The PF coils were designed in order to obtain a high compression of the SP ($\rho_{\text{Pinch}}(0)/R_{\text{sph}} \approx 0.1$) and the high elongation of the ST ($\kappa \approx 2.3$); this should allow one to obtain a spherical-tokamak-like safety factor profile inside the ST: $q_0 \approx 1$ and $q_{95} \approx 3$ during the whole compression phase. The equilibrium calculations show that the formation and compression of PROTO-SPHERA is quite robust and resilient to large changes in the internal plasma profiles, which can be controlled by limited changes in the current of the compression PF coils.

For the sustainment phase, numerical calculations [14] using the principle of minimum energy dissipation, with the constraint of helicity balance, show that monotonically increasing q -profiles (typical of spherical tokamaks) can be obtained inside the FCS surrounded by flux conserver, if the electrical resistivity is minimum at the symmetry axis and if the ratio between the constant relaxation parameter μ_{SP} in the SP and the volume averaged relaxation parameter $\langle \mu \rangle_{ST} = \mu_0 \langle \vec{j} \cdot \vec{B} / B^2 \rangle_{ST}$ in the ST is in the range $2 \leq \mu_{SP} / \langle \mu \rangle_{ST} \leq 4$. Whether this safety factor profile is compatible with sustainment through magnetic relaxation (for an equilibrium supported by PF coils and in the absence of a flux conserver near the plasma) remains an open question [27] to be settled by the experiment, along with a number of other questions, which mainly deal with the physics at the interface between the ST and the SP.

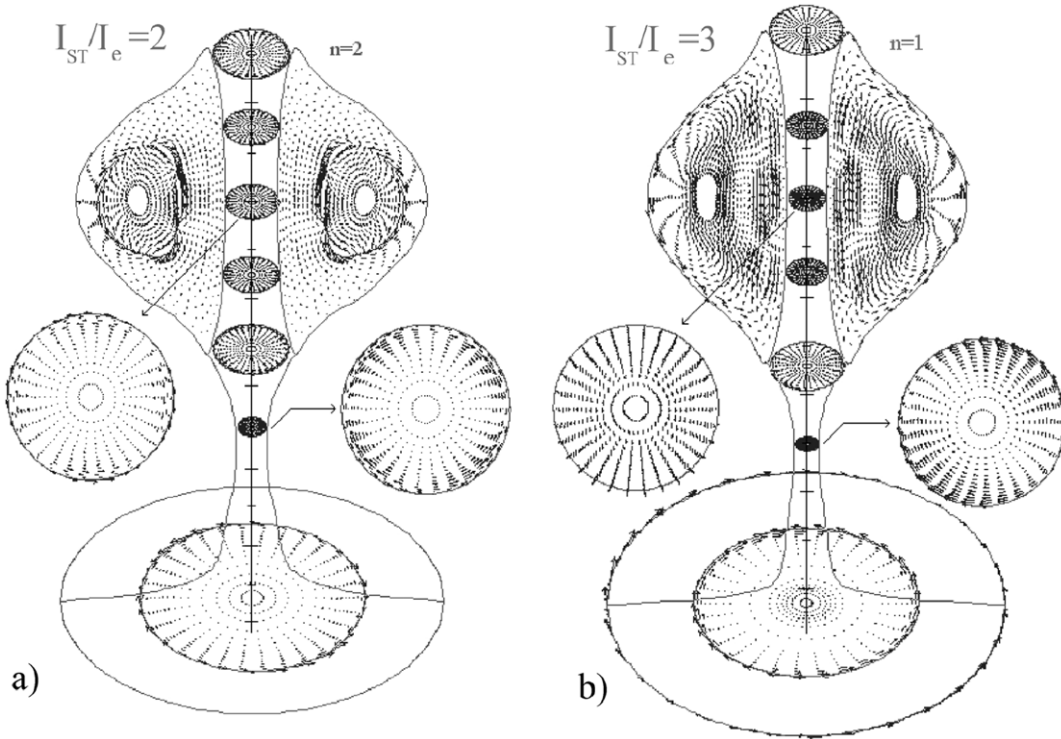


Figure 11. Displacement arrow plots for PROTO-SPHERA at $I_e = 60$ kA: (a) $n = 2$ unstable with $I_{ST} = 2I_e = 120$ kA, $\beta_{ST} \approx 25\%$ and standard profiles (4); (b) $n = 1$ unstable with $I_{ST} = 3I_e = 180$ kA, $\beta_{ST} \approx 33\%$ and modified profiles (see the appendix), with $h = 0.9$, $\Delta\mu/\mu_{edge} = 0.5$.

The ideal MHD stability properties of PROTO-SPHERA were calculated by a new finite element stability code. The result is that the most relevant parameter is the ratio I_{ST}/I_e : the configuration is ideal MHD stable up to a plasma beta in the ST $\beta_{ST} \sim 25\text{--}30\%$ at $I_{ST}/I_e \leq 1$, but only up to $\beta_{ST} \sim 14\text{--}16\%$ at $I_{ST}/I_e \sim 4$. At low ratio I_{ST}/I_e and at low β_{ST} the dipole moment of the divertor PF coils, which provide the disc shape in front of the electrodes, is aligned (stabilizing) with the ST dipole moment and dominates over the opposite (destabilizing) dipole moment of the compression PF coils and therefore stabilizes the ST tilt instability. At high β_{ST} the ST tilt instability is destabilized by an increased opposite dipole moment of the compression PF coils. At a high ratio I_{ST}/I_e the SP becomes kink unstable, due to its strong compression $\rho_{pinch}(0)/R_{sph} \leq 0.1$, and destabilizes the tilt of the ST.

The three major points that will be investigated on the PROTO-SPHERA experiment are whether the formation and compression scheme is effective and reliable, whether the combined configuration can be sustained in ‘steady-state’ by dc helicity injection (in the absence of a closed flux conserver near the ST) and finally how the energy confinement compares with the one measured on spherical tokamaks.

The MULTI-PINCH experimental setup is under construction in Frascati inside the START vacuum vessel: its design philosophy is such that, if the results concerning the SP breakdown and stability are satisfactory, PROTO-SPHERA can be obtained with a modular implementation of this experimental setup.

Appendix. Resilience of the PROTO-SPHERA equilibria to changes of the internal profiles

Any single PF coil of PROTO-SPHERA can be connected in principle to a dedicated power supply, but in practice it would be extremely difficult to provide an active equilibrium feedback during the fast formation phase (≈ 1 ms). The consequent choice of subdividing the PF coils in two groups, each composed of coils connected in series (see figure 3), reduces the versatility of the experiment and therefore compels us to assess the resilience in the free boundary equilibria to the changes of the internal plasma profiles.

The SP must be an inhomogeneous force-free plasma, due to the open nature of its flux surfaces, but the stronger hypothesis of equation (3) that the relaxation parameter $\mu(\psi)$ is also constant inside the SP (homogeneous force-free plasma) can be removed. The first investigation of the equilibrium resilience, while keeping the functional forms of $p(\psi)$ and $f(\psi)$ unchanged inside the ST, introduces, inside the SP, a power exponent upon the normalized poloidal current:

$$f(\psi) = (\mu_0 I_e / 2\pi) (\psi / \psi_X)^{\alpha/2}, \quad (\text{A1})$$

with $\alpha = 2$ representing the homogeneous force-free plasma of equation (3). The result is that, in spite of large variations in the plasma current distribution internal to the SP ($\alpha = 1.5$ to $\alpha = 3$), the disc-shaped regions of the SP always fit the electrodes, mainly because the ST elongation does not depend upon the power exponent α .

The second investigation of the equilibrium resilience is that of varying the functions $p(\psi)$ and $f(\psi)$ inside the ST, while assuming that the SP is a homogeneous force-free plasma ($\alpha = 2$). The chosen parametric form is the one used for

the Chandrashekar–Kendall–Furth (CKF) configurations [29], with the pressure profile such that the largest $\bar{\nabla}p$ coincides with the largest $\bar{\nabla}\langle\mu\rangle$:

$$\begin{aligned}
 p(\psi) &= p_{\text{edge}} = \text{constant} && \text{for } \psi < \psi_X \quad (\text{SP}), \\
 p(\psi) &= p_{\text{edge}} \cdot \left\{ 1 + (\Delta p/p_{\text{edge}}) \right. \\
 &\quad \cdot \left. \left[1 - \cos\left(\frac{\pi(\psi - \psi_X)}{(\psi_c - \psi_X)}\right) \right] \right\} && \text{for } \psi_X \leq \psi \leq \psi_c \quad (\text{ST}), \\
 p(\psi) &= p_{\text{edge}} \cdot \{1 + (\Delta p/p_{\text{edge}})\} && \text{for } \psi > \psi_c \quad (\text{ST}).
 \end{aligned} \tag{A2}$$

The normalized poloidal current $f(\psi)$ is

$$\begin{aligned}
 2\pi f(\psi) &= \mu_{\text{SP}}\psi \quad \text{for } \psi < \psi_X \quad (\text{SP}), \\
 2\pi f(\psi) &= (\mu_{\text{SP}} - \mu_{\text{edge}})\psi_X + \mu_{\text{edge}} \left\{ \psi + \frac{2}{\pi} \left(\frac{\Delta\mu}{\mu_{\text{edge}}} \right) \right. \\
 &\quad \times (\psi_c - \psi_X) \left[\cos\left(\frac{\pi(\psi - \psi_X)}{2(\psi_c - \psi_X)}\right) - 1 \right] \left. \right\} \\
 &\quad \text{for } \psi_X \leq \psi \leq \psi_c \quad (\text{ST}), \\
 2\pi f(\psi) &= (\mu_{\text{SP}} - \mu_{\text{edge}})\psi_X + \mu_{\text{edge}} \left\{ \psi_c - \frac{2}{\pi} \left(\frac{\Delta\mu}{\mu_{\text{edge}}} \right) \right. \\
 &\quad \times (\psi_c - \psi_X) + \left. \left(1 - \frac{\Delta\mu}{\mu_{\text{edge}}} \right) (\psi - \psi_c) \right\} \\
 &\quad \text{for } \psi > \psi_c \quad (\text{ST}).
 \end{aligned} \tag{A3}$$

The dimensionless parameter h ($0 \leq h \leq 1$) controls the width of the profiles: both $\bar{\nabla}p$ and $\bar{\nabla}\langle\mu\rangle$ are concentrated in the interval $\psi_X \leq \psi \leq \psi_c$, with

$$\psi_c = \psi_X + h(\psi_{\text{max}} - \psi_X). \tag{A4}$$

The parameter $\Delta\mu$ represents the drop in the relaxation parameter from the edge to the axis of the ST plasma: $\Delta\mu = \mu_{\text{edge}} - \mu_{\text{axis}}$, and the parameter Δp the drop in the kinetic pressure from the axis to the edge of the ST plasma: $\Delta p = p_{\text{axis}} - p_{\text{edge}}$. The relaxation parameter $\mu(\psi)$ takes inside the SP the constant value

$$\mu_{\text{SP}} = \mu_0 I_c / \psi_X; \tag{A5}$$

it jumps to the value μ_{edge} at the edge of the ST, then decreases to $(\mu_{\text{edge}} - \Delta\mu)$ in the interval $\psi_X \leq \psi \leq \psi_c$ and finally remains constant at this value between ψ_c and the ST magnetic axis ψ_{max} .

Given the same current in the Group ‘A’ PF compression coils, the PROTO-SPHERA formation sequence computed with a peaked pressure profile— $h = 0.9$ and $(\Delta\mu/\mu_{\text{edge}}) = 0.5$ —is characterized by $q_0 \approx 2$ – 2.5 , in contrast with the formation sequence computed with the standard profiles of equation (4), which has $q_0 \approx 1$. Nevertheless, the major difference is just the outer radius of the ST, which is smaller by only 3 cm in the former case ($R_{\text{sph}} \approx 34$ cm) with respect to the latter case ($R_{\text{sph}} \approx 37$ cm); very slight differences (3 mm) are instead obtained for the inner radius of the ST, $\rho_{\text{Pinch}(0)}$.

Table A1 summarizes the result that the scan of the parameters h and $(\Delta\mu/\mu_{\text{edge}})$ has upon the 180 kA case. It is to be noted that in table A1 the current of the compression PF coils of Group ‘A’ was slightly changed, under the constraint of keeping as constant as possible the ST external radius R_{sph} , exactly at the value obtained with the choice $h = 0.9$, $(\Delta\mu/\mu_{\text{edge}}) = 0.5$: i.e. $R_{\text{sph}} \approx 32$ cm. The case with the standard functional forms (4) has instead a larger

Table A1. PROTO-SPHERA parameters at the time-slice corresponding to $I_{\text{ST}} = 180$ kA, computed with various choices for the forms of $p(\psi)$ and $f(\psi)$: standard form means equation (4), whereas the forms with parameters h and $\Delta\mu/\mu_{\text{edge}}$ refer to equations (A2–A4).

p and f form	$I_{\text{A}'} [\text{A}]$	$R_{\text{sph}} [\text{cm}]$	$\rho_{\text{Pinch}}(0) [\text{cm}]$	q_{95}	q_0
Standard	898	35.9	4.1	2.57	0.96
$h = 0.9,$ $\Delta\mu/\mu_{\text{edge}} = 0.5$	898	32.3	4.1	3.15	2.27
$h = 0.3,$ $\Delta\mu/\mu_{\text{edge}} = 0.5$	875	31.7	5.1	2.71	1.35
$h = 0.9,$ $\Delta\mu/\mu_{\text{edge}} = 0.2$	922	32.2	3.6	3.19	1.82
$h = 0.9,$ $\Delta\mu/\mu_{\text{edge}} = 0.8$	859	32.1	5.3	2.84	3.31

$R_{\text{sph}} \approx 36$ cm. The required plasma shape can be reasonably matched with variations in the current $I_{\text{A}'}$ smaller than 5%.

References

- [1] Post R.F. and Santarius J.F. 1992 *Fusion Technol.* **22** 13
- [2] Alladio F. *et al* 2001 PROTO-SPHERA ENEA Serie Energia Associazione Euratom-ENEA sulla Fusione RT/ERG/FUS/2001/14
- [3] Jensen T.H. and Chu M.S. 1980 *J. Plasma Phys.* **25** 459
- [4] Taylor J.B. and Turner M.F. 1989 *Nucl. Fusion* **29** 219
- [5] Sykes A. *et al* 1992 *Nucl. Fusion* **32** 694
- [6] Alladio F. *et al* 2000 Results of proto-pinch testbench for the Proto-Sphera experiment *Proc. 27th Eur. Conf. (Budapest, 2000)* vol 24B (Europhys. Conf. Abstract) p 161
- [7] Amemiya N. *et al* 1991 *J. Phys. Soc. Japan* **60** 2632
- [8] Amemiya N. *et al* 1993 *J. Phys. Soc. Japan* **63** 1552
- [9] Taylor J.B. 1974 *Phys. Rev. Lett.* **33** 1139
- [10] Berger M.A. and Field G.B. 1984 *J. Fluid Mech.* **147** 133
- [11] Boozer A.H. 1986 *Phys. Fluids* **29** 4123
- [12] Rosenbluth M.N. and Bussac M. 1979 *Nucl. Fusion* **19** 489
- [13] Tang X.Z. *et al* 2005 Physics design bases of a spherical torus with a plasma center column *American Physical Society, 47th Annual DPP Meeting (Denver, CO, USA, October 24-28, 2005)* abstract #RP1.058 <http://meetings.aps.org/Meeting/DPP05/Event/36080>
- [14] Farengo R. and Caputi K.I. 2002 *Plasma Phys. Control. Fusion* **44** 1707
- [15] Brennan D. *et al* 1999 *Phys. Plasmas* **6** 4248
- [16] Nelson B.A. *et al* 1995 *Phys. Plasmas* **2** 2337
- [17] Stallard B. W. *et al* 2003 *Phys. Plasmas* **10** 2912
- [18] Alladio F. and Micozzi P. 1997 *Nucl. Fusion* **37** 1759
- [19] Rogier F. and Mancuso A. 2004 *Int. J. Comput. Eng.* **5** 1
- [20] Alladio F. *et al* 2005 *Phys. Plasmas* **12** 112502
- [21] Marsh G.E. 1996 *Force-free Magnetic fields Solutions, Topology and Applications* (Singapore: World Scientific)
- [22] D’haeseleer W.D. *et al* 1991 *Flux Coordinates and Magnetic Field Structure* (Berlin: Springer)
- [23] Lackner K. and Gottardi N.A.O. 1990 *Nucl. Fusion* **30** 767
- [24] Greenwald M. *et al* 1988 *Nucl. Fusion* **28** 2199
- [25] Sweet P.A. 1958 *Nuovo Cimento Suppl.* **8** SerX 1888
- [26] Parker E.N. 1963 *Astrophys. J. Suppl. Ser.* **8** 177
- [27] Sovinec C.R. *et al* 2001 *Phys. Plasmas* **8** 475
- [28] Alladio F. *et al* 2004 Ideal MHD stability calculations in presence of magnetic separatrices *12th Int. Congr. on Plasma Physics: ICPP 2004 (Nice, France)* <http://hal.ccsd.cnrs.fr/ccsd-00001811>
- [29] Rogier F. *et al* 2003 Simply Connected High- β Magnetic Configurations *11th Int. Congr. on Plasma Physics: ICPP 2002 (Sydney, Australia)* *American Institute of Physics* vol **669** p 557